Research Article **www.ijcps.com**

International Journal of Chemical and Pharmaceutical Sciences
2014, Dec., Vol. 5 (4)

ISSN: 0976-9390
IJCPS

Effect of side chain substituents on the geometrical pattern of some newly synthesized perylene tetracarboxylic diimides using DFT Calculations

Andrea Sandra Christine D'Cruz and Sankaran KR*.

Department of Chemistry, Annamalai University, Annamalainagar, India.

***Corresponding Author:** E-Mail: professorkrs60@gmail.com

Received: 21 Dec 2014, Revised and Accepted: 29 Dec 2014

ABSTRACT

The synthesis of a newly synthesized perylene tetracarboxylic diimide (PTCDI) study reports the effect of the different side chain substituent on the optimized and geometrical features of the compound. Geometrical parameters such as NMR shielding, HOMO-LUMO and molecular electrostatic potentials (MEP) of the compound were elucidated to determine its structural properties. The morphological features for the compounds were carried by using various microscopic techniques such as scanning electron microscopy (SEM) and phase contrast microscopic techniques and are discussed here.

Keywords: PTCDI; NMR shielding; HOMO-LUMO; MEP; SEM; phase contrast microscopy.

1. INTRODUCTION

PTCDIs are an important class of pigments known to exhibit very good chemical, thermal and photochemical stability [1]. They also relatively show high electron affinities, excellent light stability, high luminescence efficiency as well as good quantum yields of fluorescence [2]. Besides this they also exhibit high molar absorbtivity, good charge and energy transport properties [3]. Their remarkable electrochemical properties makes them suitable candidates as electron acceptors and electron transporting materials. Horowitz *et al.* in 1996 demonstrated good charge transport properties in N,N'-diphenyl-3,4,9,10-perylenetetracarboxylic-diimide [4]. From previous literature studies we observe that the high electron transport performance can be attributed to two main factors. Firstly high electron affinities and low LUMO energy levels does not only help electron injection from contacting electrodes but also enhances their air stabilities. Secondly it helps in easy formation of π-π packing, which improves better neighbouring intermolecular electronic orbital couplings and thus improve electron mobilities [5]. Another interesting feature of PTCDIs is that their emission colour can be tuned from red to black [6]. The reason is that perylene derivatives in the solid state can form a number of polymorphs or phases containing varying colours which is due to the intermolecular electronic interactions of the closed packed molecules [7]. Hence their role as red vat dyes and pigments were of prominent importance due to its good light and weather fastness, excellent thermal stability and chemically inertness properties [8]. An intriguing property of PTCDIs is that they demonstrate good self-assembly behaviour due to its strong π-π stacking. The packing of solid PTCDIs has been exclusively carried out for use in organic electronics applications where good intermolecular orbital overlap is related to charge-carrier mobility [9]. Thus well developed organic devices can be designed because of the strong π-π interactions between the planar PTCDI rings. Self-aggregation of PTCDIs are generally studied by their absorption and emission properties as they show strong absorption in the UV-vis region [10]. Another reason why PTCDIs is highly preferred is because of its low cost and availability [3]. They are thus widely used for electronic materials such as photovoltaic cells, optical switches, lasers, organic solar cells (OSCs), intense photoluminescence, organic light emitting diodes (OLEDs), organic field effect transistors (OFETs), dye lasers, sensors, liquid crystalline materials and molecular switches and so forth [11-15]. The main disadvantage of PTCDIs lies with their insolubility in many organic solvents. This can however be overcomed by substitution at either the imide or bay positions. Substitution at the imide position does not change the optical properties, but substitution at the bay position does alter the optical properties of the compounds due to increased steric hindrance which in turn

affects the self-organization. The steric hindrance of the substituent side chains are thus known to excercise influence on the π-π intermolecular stacking of the PTCDI core by having an impact on the solubility, the aggregation and the electron mobility of the material in the solid state. Thus it is a known fact that the choice of side chains play an important role in determining the molecular packing, morphology, colouration and thus enhancing the optoelectronic properties of the PTCDIs. The aim of this paper is to understand the molecular structure of the synthesized compound at the molecular level using computational studies.

2. MATERIALS AND METHODS

2.1. Materials used

Perylene-3,4,9,10-tetracarboxylic dianhydride (PTCDA), 2-amino-4,6-dimethyl pyrimidine and imidazole were obtained from Sigma Aldrich, India while 2-amino pyridine was purchased from Avra chemicals , India and were used as such without any further purification.

2.2. Instrumentation

^{1}H NMR spectra in DMSO-d_6 were recorded on a Bruker 400 MHz spectrometer. Chemical shifts were measured in parts per million (ppm). Mass spectra were obtained with JEOL GCMATE 11 GC Mass spectrometer. SEM image was recorded on a JEOL INDIA Pvt. Ltd., JSM-6610LV instrument. The sample was prepared by casting a drop of the suspension dissolved in DMSO onto a clean glass slide, followed by annealing it in an oven overnight. The sample was then coated with platinum prior to the SEM measurement. Phase contrast microscopic images were obtained using a NIKON TYPE 120c, NIKON ECLIPSE TS 100 microscope by droping a suspension of the sample onto a clean glass slide followed by drying in air. Water contact angles were measured using a Drop Shape Analyzer (DSA) (Kru ¨ss GmbH Germany).

2.3. Experimental

Langhals *et al.,* were the first to mention about the synthesis of PTCDIs. We have carried out the synthesis using perylene tetracarboxylic dianhydride (PTCDA; 0.395 g, 1 mmol) and a primary amine in the presence of a suitable catalyst such as molten imidazole (6 g) taken in a 50 mL round bottom flask and made to undergo condensation reaction for a period of 4h at 160-180°C. After completion of the reaction, the reaction mixtures were further treated with 100 mL ethanol and 300 mL 2M HCl and was kept to stir overnight. On completion of the stirring process the precipitate was washed with copious amount of water until the washings turned neutral. The compound were then dried, weighed and then characterized for further studies. In this paper we have synthesized two compounds namely as N,N'-Bis(2-amino-4,6-dimethyl pyrimidine)perylene-3,4,9,10-tetracarboxylic diimide (AD-PTCDI), N,N'-Bis(2-aminopyridine)perylene-3,4,9,10-tetracarboxylic diimide (AP-PTCDI) using 2-amino-4,6-dimethyl pyrimidine (0.246 g, 2 mmol) and 2-aminopyridine (0.188 g, 2 mmol) respectively.

AD-PTCDI: ^{1}H NMR (400MHz, DMSO-d_6): δ 2.5 (s, 17H, CH_3), 7.6 (s, 2H, Ar-pyrimidine), 7.95 (d, 2H, perylene, J=8Hz), 8.25 (d, 2H, perylene, J=8Hz); IR (KBr, cm^{-1}): υ 3422, 2960, 2922, 2847, 1676, 1646, 1589, 1562, 1427, 1362, 1267, 1244, 1113, 1050, 1030, 872, 835, 809, 728, 653; MS(EI): m/z calcd, for $C_{36}H_{22}N_6O_4$, 602.1; Found: 602.6; yield: 70%.

AP-PTCDI: IR (KBr, cm^{-1}): υ 3426, 2923, 2844, 2365, 1687, 1592, 1432, 1352, 1097, 802, 650, 546, 493; MS(EI): m/z calcd, for $C_{34}H_{16}N_40_6$, 544.1; Found: 544.5 [M$^+$]. Solid fluorescence: λ_{max} ~ 609 (nm) (λ_{exc}=460 nm); yield: 70%.

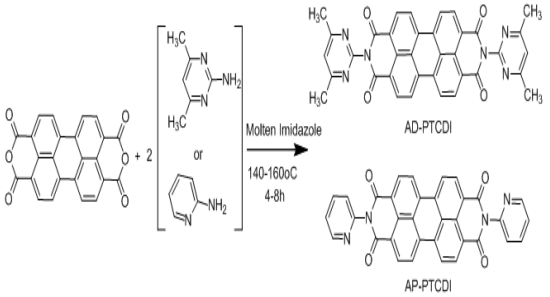

Scheme - 1: Synthesis of PTCDI.

3. RESULTS AND DISCUSSION

PTCDIs are of significant interest as they demonstrate high electron affinities, large electron mobility, excellent thermal and oxidative stabilities, high molar absorptivities, and good quantum yields of fluorescence.

3.1. NMR and NMR shielding

From the ^{1}H NMR spectrum for compound AD-PTCDI, as seen in figure 1. It can be observed that the distribution of protons is clearly well spread. The methyl peak appeared as a singlet at 2.50 ppm. The aromatic perylene ring exists as two distinct doublets in the regions 7.95 and at 8.25 ppm respectively. The pyrimidine aromatic proton appeared at 7.60 ppm. The formation of the compound was supported by mass spectral data (MS-EI) which was found to be in good agreement with the calculated value (S1). On the other hand very few studies have been reported of the use of heterocyclic compounds such as pyridine, imidazole, triazole,

anthraquinone *etc* on the synthesis and self-assembly of PTCDIs although they are known to exhibit fascinating properties such as forming hydrogen bonds which in turn are known to affect the self-assembly and opto-electronic properties of the materials. They are thus known to serve as challenging substituents for promising applications in the scientific industry [16,17]. J. Sun *et al.* synthesized a series of PTCDIs containing several pyridine N-oxide groups which were attached to the aromatic chromophore (perylene core or to imide groups) and which exhibited high fluorescence and good water solubility **[18]**.

Here in our study, ^{1}H NMR spectra, however, could not be recorded for compound AP-PTCDI due to its poor solubility in common organic solvent. Nonetheless the formation of the compound was determined by MS-EI analysis which was found to be consistent with the calculated values (S1).

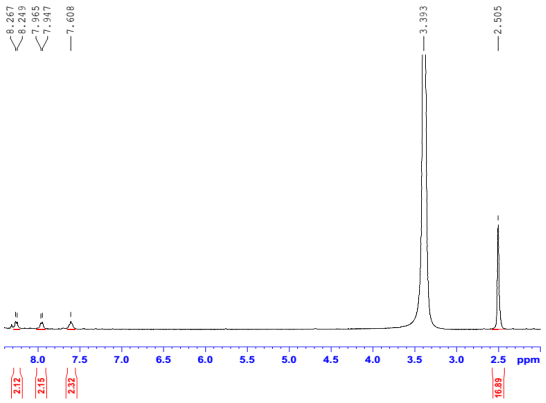

Figure – 1: ^{1}H NMR spectrum of AD-PTCDI.

3.2. Solid UV-vis and fluorescence studies

The synthesized compounds were insoluble in a vast major of organic solvents and hence its photophysical studies could not be recorded in the solution state. Thus their optical properties were carried out in the solid state and the band gap were calculated. From Fig 2, it can be clearly seen that the solid state UV-vis spectra for the synthesized compounds totally differs from that of those compounds recorded in the solution state with respect to their wavelength range and peak positions due to solid state aggregation and also because of its amorphous nature [19]. Band gap energies were calculated using The Kubelka–Munk algorithm [20].

$$F(R) = (1 - R)^2 / 2R = \alpha/s = Ac/s$$

where F(R) is Kubelka – Munk fuction, R is the reflectance of the crystal, α is the absorption coefficient and s is scattering coefficient, A is the absorbance and c is concentration of the absorbing species and h*v* is the photon energy [21]. The optical band gap for AP-PTCDI and AD-PTCDI was found to be 5.82 and 5.71 eV, respectively (Figure 2) as calculated from the absorption band in the solid state. The higher band gap value is due to the different side chain substituents. The difference is mainly attributed to the methyl groups present in AD-PTCDI which is absent in AP-PTCDI. Literature studies in small organic conjugated molecules revealed that as the band gap increases, the exciton binding energy also increases. This is normally observed in the increasing ordering of PTCDIs that eventually leads to an increase in the exciton diffusion length and also helps in the improvement in the charge carrier mobilities. It is a known fact that the solid state packing plays an important role in the determining the performance efficiency of the device [22,23].

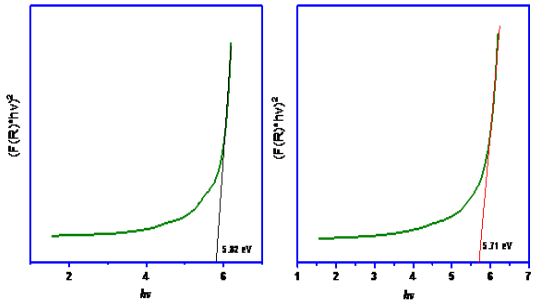

Figure – 2: Tauc plots for AD-PTCDI and AP-PTCDI.

The fluorescence spectra of the synthesized compounds in solid state were found to be quite different as compared to the sharp and well defined peaks as seen in the solution state for the other synthesized compounds of PTCDIs as reported elsewhere in literature. Here in the solid state, the fluorescence maximum of both of the synthesized compounds AP-PTCDI and AD-PTCDI no distinguishable shoulder peak corresponding to the S_0-S_2 transitions as observed in the solution state were seen which was due to the large red shift in emission (~ 609 nm) indicated the presence of pronounced intermolecular interactions such as changes in molecular stacking (π-π interactions) [24]. This is also due to the high degree of order, which are associated with large exciton diffusion lengths and high charge carrier mobilities [25]. The red shift in the fluorescence spectra also acts as another indication of the formation of aggregates. Whereas, a blue shift of effective excitation wavelength in the solid state can be attributed to the effective absorption transition from ground state to higher excited state [26]. However, minor variations on the fluorescence intensity for both of the synthesized compounds were observed. From the figure 3, we

can see that the emission intensity increases with the use of different substituent's.

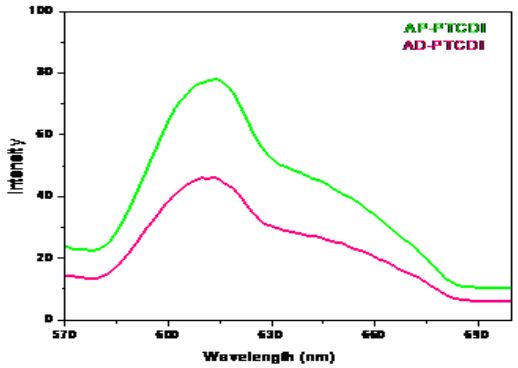

Figure - 3: Solid fluorescence spectral images of AD-PTCDI and AP-PTCDI.

3.3. Microscopic measurements

The surface morphological features of the synthesized compounds (solid powder) were characterized by SEM and phase contrast microscopy techniques. SEM images showed small cluster like formation as seen in figure 3. Phase contrast microscopy images revealed small short black rods for compound AD-PTCDI while small and thin black rods were observed for compound AP-PTCDI as seen in figure 4. The rod like features are due to the π-π stacking configuration and also because of its side chain which helps prevent molecules from assembling along a one dimension [27].

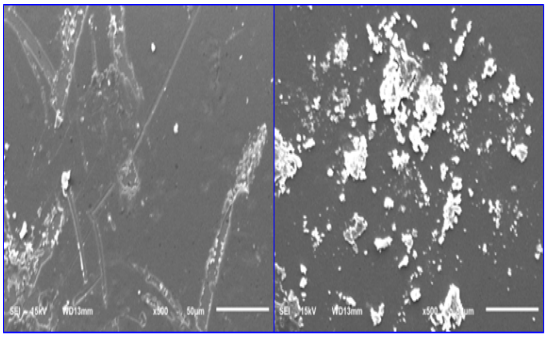

Figure – 3: SEM images of AD-PTCDI and AP-PTCDI.

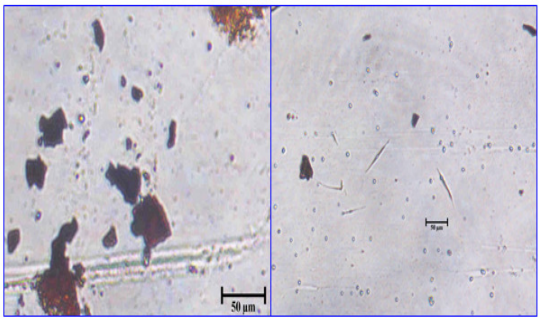

Figure - 4: Phase contrast microscopic images of AD-PTCDI and AP-PTCDI.

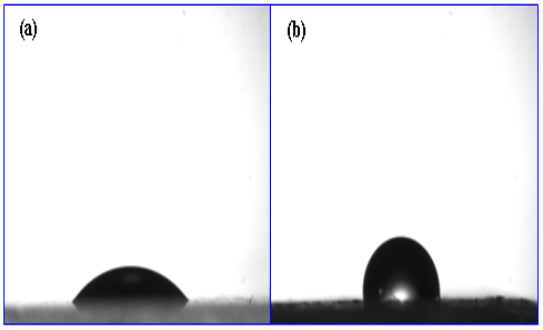

Figure – 5: Phase contrast image of (a) AD-PTCDI (b) AP-PTCDI.

3.4. Water contact angle measurements

Water contact angle test is an important parameter in determining the wettability nature of the compound *.ie.* to identify whether the material is hydrophobic or hydrophilic in nature. A material is considered to be hydrophobic in nature if it shows a contact angle above than 90°. On the other hand if the contact angle is below than 90° then the material is considered to be hydrophilic in nature. However if the contact angle reaches an upper higher limit of 180°, then the material it is termed to be superhydrophobic in nature. Hydrophobic surfaces are mainly dependent on some primary parameters such as surface roughness and low surface energy [**28**]. Lotus leaf is a perfect natural example which exhibits super hydrophobic property. It is mainly used for self-cleaning applications. Other such leaves which shows such intriguing property are *Brassica oleracea, Eryngium ebracteatum and Colocasia esculenta* [29]. This can be supported by the work carried out by Kerstin Koch who studied the hydrophobicity of plant surfaces by noting its structure and morphology features as well as carrying out experimental work related to the wetting properties [30].

Polarity of a solvent also plays a crucial key in determining the hydrophobic as well hydrophilic property of the materials. Figure 5a, b shows image of water droplet for compounds AP-PTCDI and AD-PTCDI respectively. The water drop contact angle for these coatings was found to be 97.992 ± 1 and 43.081 ± 1 respectively. The increase in the contact angle indicates that there is an increase in hydrophobicity of the nature of the compound. Hence, here in this work it can be clearly observed that compound AP-PTCDI is more hydrophobic in nature as compared to its counterpart compound AD-PTCDI and hence can be used for self- cleaning applications.

3.5. Computational studies

The main objective for performing out computational studies is to understand the

relationship between the optical properties and the structure modifications of PTCDI molecules. In this work, all of the calculations were carried out using Gaussian package.

3.5.1. HOMO-LUMO

The HOMO is the ability to donate an electron, whereas LUMO acts as an electron acceptor. The electron acceptor character is an important feature observed in PTCDIs which arises from the strong electron-withdrawing nature of the imides groups. Addition of a second electron into the next LUMO, almost equivalent to the addition of an electron into the second imide group, can involve a lower energy [31]. PTCDIs also show a direct band gap [32]. The energy gap of PTCDIs between the HOMOs and LUMOs, is a critical parameter in determining molecular electrical transport properties because it is a measure of electron conductivity as well as determines the molecular chemical stability. The chemical hardness is a good indicator of the chemical stability [33-36]. The energy gaps were observed to be 2.59 and 2.8 eV for AD-PTCDI and AP-PTCDI respectively. Graphical images of HOMO-LUMO energy gaps were displayed in figure 5.

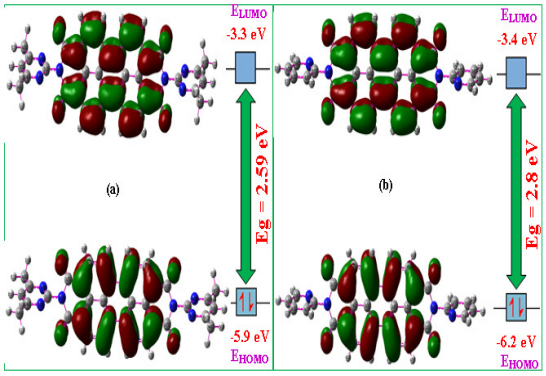

Figure – 5: HOMO-LUMO energy gaps (a) AD-PTCDI (b) AP-PTCDI.

3.5.2. Molecular electrostatic potential (MEP)

MEP analysis is used to identify the molecular size and the positive, negative or neutral electrostatic potential of the compounds by using the colour scale. In MEP, red colour indicates electrophilic reactivity while blue colour denotes nucleophilic reactivity. Hence it is a powerful tool to identify the regions that will undergo electrophilic or nucelophilic attack [37-41]. Thus this method is found to be beneficial in elucidating the molecular structure of the synthesized compounds. The different values of the electrostatic potential are represented by different colours. Red colour indicates the more reactive. Graphical image of MEP is displayed in figure 6.

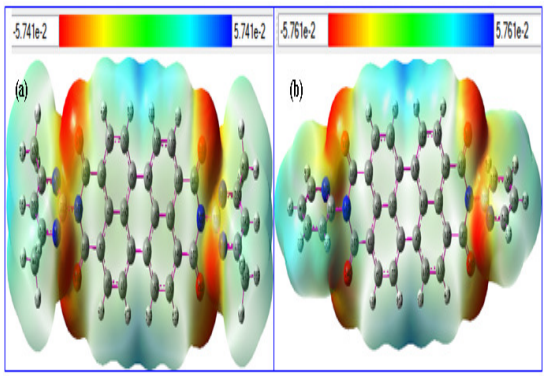

Figure – 6: MEP images of (a) AD-PTCDI (b) AP-PTCDI.

4. CONCLUSIONS

Here in this study carried the synthesis of two newly synthesized PTCDIs. The rod like morphological features revealed that these compounds are suitable to be used for the design of new organic devices, while its water contact angle measurements showed that compound AP-PTCDI exhibited good hydrophobic behaviour and thus could be used for self-cleaning application purposes in the organic electronic industry. Computational studies such as NMR shielding, HOMO-LUMO and molecular electrostatic potential (MEP) analysis were performed in order to derive information regarding charge transfer within the molecule. The calculated HOMO-LUMO energy gap readings revealed that the synthesized compounds exhibits chemical activity as well as kinetic stability within the molecule. MEP diagram also confirmed the presence of electrophilic and nucleophilic sites for the compounds.

5. REFERENCES

1. José A. Quintana, José M. Villalvilla, Alejandro de la Pe a, Jos L. Segura, and María A. Díaz-García**. J. Phys. Chem. C,** 2014; 118: 26577 –26583.
2. Ymene Houari, Adele D. Laurent, and Denis Jacquemin. **J. Phys. Chem. C,** 2013; 117: 21682 –21691.
3. Dominik W. Gehrig, Steffen Roland, Ian A. Howard, Valentin Kamm, Hannah Mangold, Dieter Neher, and Frede ric Laquai. **J. Phys. Chem. C, 2014;** 118: 20077–20085.
4. Horowitz G, Kouki F, Spearman P, Fichou D, Nogues C, Pan X and Garnier F. **Adv. Mater,** 1996; 8: 242
5. Yun Geng, Hai-Bin Li, Shui-Xing Wu and Zhong-Min Su. **J. Mater. Chem.,** 2012: 22: 20840.

6. Herbst W and Hunger K. Industrial Organic Pigments, 2nd Ed VCH, Weinheim, 1997.
7. Sheng Gao Liu, Guodong Sui and Russell A. Cormier, Roger M. Leblanc and Brian A. Gregg, **J. Phys. Chem. B,** 2002; 106: 1307-1315.
8. Eva M. Calzado, Jose M. Villalvilla, Pedro G. BojJose A. Quintana, Rafael Go mez, Jose L. Segura and Marı a A. Dı az-Garcı. **J. Phys. Chem. C,** 2007; 111: 13595-13605.
9. Chun Huang, Stephen Barlow, and Seth R. **Marder J. Org. Chem.** 2011; 76: 2386–2407.
10. Pieter AJ. De Witte, Jordi Hernando, Edda E. Neuteboom, Erik M. H. P. van Dijk, Stefan C. J. Meskers, Rene A. J. Janssen, Niek F. van Hulst, Roeland J. M. Nolte, Maria F. Garcı´a-Parajo and Alan E. Rowan, **J. Phys. Chem. B,** 2006; 110: 15.
11. Dennler G, Scharber MC and Brabec C. **J. Adv. Mater. 2009;** 21: 1323–1338.
12. Thompson BC and Frechet JM. **J. Angew. Chem. Int. Ed.** 2008; 47: 58–77.
13. Mishra A, Fischer MKR and Bäuerle P. **Angew. Chem., Int. Ed. 2009;** 48: 2474-2499
14. Fischer A and Bäuerle MKR. **P. Angew. Chem., Int. Ed.** 2009; 48: 2474-2499.
15. Li, C, Liu, M, Pschirer, NG, Baumgaten, M and Müllen K. **Chem. Rev.** 2010; 110: 6817-6855.
16. Bo Yang, Feng-Xia Wang, Kai-Kai Wang,a Jing-Hui Yan, Yong-Qiang Liua and Ge-Bo Pan. **Phys. Chem. Chem. Phys.,** 2014; 16: 25251-25254.
17. Xuejun Zhan, Ji Zhang, Sheng Tang, Yuxuan Lin, Min Zhao, Jie Yang, Hao-Li Zhang, Qian Peng, Gui Yu and Zhen Li. **Chem. Commun.,** 2015; 51: 7156—7159.
18. Juanjuan Sun, Ming Wang, Ping Xu, Shuai Zhang, and Zhiqiang Shi. **Synthetic Communications,** 2012; 42: 1472–1479.
19. Sivamurugan Vajiravelu, Lygaitis Ramunas, Gra zulevi cius Juozas Vidas, Gaidelis Valentas, Jankauskas Vygintasc and Suresh Valiyaveettil. **J. Mater. Chem.,** 2009; 19: 4268–4275
20. Kubelka P, Munk F and Ein Beitrag zur Optik der Farbanstriche. **Z. Tech. Phys. (Leipzig),** 1931; 12: 593–601.
21. Aditya Prasad A and Meenakshisundaram SP. **J. Appl. Cryst.** 2015; 48: 844–852.
22. Andre Wicklein, Andreas Lang, Mathis Muth, and Mukundan Thelakkat. **J. Am. Chem. Soc.** 2009; 131: 14442–14453.
23. Jancy B and Asha SK. **Chem. Mater.** 2008; 20: 169–181.
24. Nisha V. Handa, Laura D. Shirtcliff, Barry K. Lavine, Douglas R. Powell, and Darrell Berlin K. **Phosphorus, Sulfur, and Silicon,** 2014; 189: 738–752.
25. Ping Yan, Arindam Chowdhury, Michael W. Holman, and David M. **Adams, J. Phys. Chem. B,** 2005; 109: 724-730.
26. Yong-Shan Ma , Chen-Hui Wang, Ying-Jie Zhao, Ying Yu, Ci-Xiang Han, Xin-Jian Qiu and Zhiqiang Shi. **Supramolecular Chemistry,** 2007; 19: 141–149.
27. Gopal Boobalan, Predhanekar Mohamed Imran, Samuthira Nagarajan, Superlattices and Microstructures. 2012; 51: 921–932.
28. Chang-Jian Weng, Chi-Hao Chang, I-Li Lin, Jui-Ming Yeh, Yen Wei, Ching-Ling Hsu and Po-Han Chen. Surface & Coatings Technology, 2012; 207: 42–49.
29. Mahendra S. Kavale, Mahadik SA, Mahadik D B, Parale VG, Rao AV, Vhatkar RS, Wagh PB and Gupta SC. **J Sol-Gel Sci Technol,** DOI 10.1007/s10971-012-2822-7.
30. Fang Wang Xiufang Wang Anjian Xie Yuhua Shen Wei Duan Ye Zhang Jialin Li. **Appl Phys A** 2012; 106: 229–235. DOI 10.1007/s00339-011-6566-y.
31. Sang Kwon Lee, Yanbing Zu, Andreas Hermann, Yves Geerts, Klaus Müllen and Allen. **J. Bard, J. Am. Chem. Soc.** 1999; 21: 3519.
32. Kis Z, Nis ¸ CI, Ö.F. Yüksel A and Us M. **Synthetic Metals,** 2014; 194: 193–197.
33. Ramalingam S, Periandy S, Karabacak M and Karthikeyan N. **Spectrochimica Acta Part A: Molecular and Biomolecular Spectroscopy,** 2013; 104: 337–351
34. Aditya Prasad A and Meenakshisundaram SP. **Cryst. Res. Technol.** 2015; 50(5): 395–404.
35. Aditya Prasad A, Muthu K, Meenatchi V, Rajasekar M, Agilandeshwari R, Meena K, Vijila Manonmoni J and Meenakshisundaram SP. **Spectrochimica Acta Part A: Molecular and Biomolecular Spectroscopy.** 2015;140: 311– 327.
36. Aditya Prasad A, Muthu K, Rajasekar M, Meenatchi V and Meenakshisundaram SP. **Spectrochimica Acta Part A: Molecular and Biomolecular Spectroscopy,** 2015; 135: 805 813.

37. Agilandeshwari R, Muthu K, Meenatchi V, Meena K, Rajasekar M, Aditya Prasad A and Meenakshisundaram SP. **Spectrochimica Acta Part A: Molecular and Biomolecular Spectroscopy**, 2015; 137: 383–388.

38. Muthu K, Meenatchi V, Rajasekar M, Aditya Prasad A. Meena K, Agilandeshwari R, Kanagarajan V, Meenakshisundaram SP. **J. Mol. Str.,** 2015; 1091: 210–221.

39. Fleming I. **Frontier Orbitals and Organic Chemical Reactions, John Wiley and Sons,** New York, 1976; 5

40. Rajasekar M, Muthu K, Aditya Prasad A and Meenakshisundaram SP. **J. Mol. Str.,** 2015; 1085: 147–154.

41. Aditya Prasad A, Muthu K, Rajasekar M, Meenatchi V and Meenakshisundaram SP. **Spectrochimica Acta Part A: Molecular and Biomolecular Spectroscopy,** 2015; 135: 46–54.